IOP Conf. Series: Materials Science and Engineering **159** (2016) 012014 doi:10.1088/1757-899X/159/1/012014

Evaluation of common tests for fracture characterisation of advanced high-strength sheet steels with the help of the FEA

I Peshekhodov, M Dykiert, M Vucetic and B-A Behrens

Institute of Forming Technology and Machines (IFUM), Leibniz Universität Hannover
An der Universität 2, 30823 Garbsen, Germany

E-mail: peshekhodov@ifum.uni-hannover.de

Abstract. The paper presents results of evaluation of common tests for fracture characterization of advanced high-strength sheet steels with the help of the FEA. The tests include three in-plane shear tests, two uniaxial tension tests, two plane strain tension tests and two equibiaxial tension tests. Three high-strength steels with different yield loci, strain hardening rates and strengths in three different thicknesses each were used. The evaluation was performed based on the spatial distribution of the equivalent plastic strain and damage variable in the specimen at the moment of crack initiation as well as on the time variation of the stress state at the crack initiation location. For in-plane shear, uniaxial tension and plane strain tension, no test can be unconditionally recommended as disadvantages of all studied tests in these groups cannot be neglected. However, in each of these groups, a test can be chosen, which represents an acceptable compromise between its advantages and disadvantages: the shear test on an IFUM butterfly specimen for in-plane shear, the tensile test on a holed specimen for uniaxial tension and the tensile test on a waisted specimen for plane strain tension. On the contrary, the bulge test on a circular specimen with a punch of Ø 100 mm can be unconditionally recommended for equibiaxial tension. In the future, optimisation of the studied tests for in-plane shear, uniaxial tension and plane strain tension appears to be necessary.

1. Introduction

Light-weight materials such as advanced high-strength steels with the ultimate tensile strength above 550 MPa (AHSS), aluminium and magnesium alloys as well as (fibre-reinforced) plastics are gaining more importance in the automotive industry. The main drivers of this trend are high energy costs and stringent legal regulations on CO_2 emissions during production and use of new vehicles. The share of these materials in the global car production accounted for 29 % in 2010 and is expected to grow up to 67 % by 2030 [1] as a recent study of McKinsey & Company states. The share of AHSS is expected to grow in absolute numbers from 15 % to 38 %, which is expected to be the strongest growth among the light-weight materials mentioned above. As opposed to the AHSS, the use of conventional steels with the ultimate tensile strength below 550 MPa is anticipated to fall from 52 % in 2010 to 13 % in 2030 [1]. This is believed to lead to a considerable reduction of the overall steel share in the material mix of the automotive industry from 67 % to 51 % over twenty years [1]. To slow down this decline, the steel manufactures need to work further on improvement of AHSS on one hand and on new solutions for a better exploitation of their advantageous properties in car manufacturing on the other.


Content from this work may be used under the terms of the Creative Commons Attribution 3.0 licence. Any further distribution of this work must maintain attribution to the author(s) and the title of the work, journal citation and DOI.
Published under licence by IOP Publishing Ltd

FEA-based forming and crash analysis can help to better exploit the advantageous properties of AHSS in car manufacturing. For that, a mathematical formulation of the material yielding, hardening and formability is required. Forming limit curves (FLC) have been long used to describe sheet metal formability [2]. Due to its standardised determination procedure, the FLC is valid for linear strain paths and plane stress states from uniaxial tension to equibiaxial tension. Despite these limitations, failure prediction in a sheet forming process based on the FLC provides an acceptable accuracy for deep-drawing steels and some aluminium alloys [3]. However, failure prediction based on the FLC for AHSS can be insufficient [3]. Especially for shear-dominated stress states or bending, alternative formability descriptions are required [4].

As an alternative approach to predict sheet metal failure, fracture models can be considered. According to these models, fracture initiation is predicted based on a relation between the equivalent plastic strain $\bar{\varepsilon}_{\mathrm{pl}}$ and the equivalent plastic strain at fracture $\bar{\varepsilon}^{\mathrm{f}}_{\mathrm{pl}}$ (or simply fracture strain). The fracture strain is a material property, which depends on the stress state, at which plastic deformation is accumulated. There exist many mathematical models describing the dependence of the fracture strain on the stress state [5, 6, 7]. To quantify a stress state, the stress triaxiality η and normalised Lode angle $\bar{\theta}$ are becoming frequently used in sheet metal forming and crash analysis [8, 9].

To calibrate fracture models, many different experimental procedures exist. Nonetheless, fracture strains of AHSS are scarce in literature and if found, they often differ much from one author to another for similar or even the same steel grades [10, 11, 12]. The differences in fracture strains $\bar{\varepsilon}^{\mathrm{f}}_{\mathrm{pl}}$ obtained by different authors can be explained with the fact that currently there is no consistent requirements nor recommendations concerning the geometry of the material specimens, test procedures and results analysis for their determination [13, 14].

The paper presents an FEA-based evaluation of different tests widely used for fracture characterisation of AHSS, which can be used as a basis for development of such requirements or recommendations. Since sheet steels were considered, the fracture calibration tests were limited to four characteristic plane stress states: in-plane shear, uniaxial tension, plane strain tension and equibiaxial tension. The FE models, evaluation criteria and results are introduced and discussed. At the end, a conclusion and outlook for future work are given.

2. Materials

The evaluation was performed on three different grades and three thicknesses to secure generality of conclusions. A dual-phase (DP) steel, a complex-phase (CP) steel and a press-hardening (PH) steel with the ultimate tensile strength from 600 MPa to 1500 MPa in 0.8 mm, 1.5 mm and 3.0 mm each were chosen. To model the yield behaviour, the Hill'48 yield condition and an isotropic strain-rate dependent hardening formulation were used as shown in figure 1.

To describe the fracture behaviour, the ductile shear fracture and ductile normal fracture of CrahFEM [6] were chosen. Both were combined to describe the fracture behaviour of DP600 and MB-W1500, whereas only the ductile shear fracture model was used for CP1000 since no ductile fracture model data was available for it. The shear fracture model is given by:

$$\bar{\varepsilon}^{\mathrm{f}}_{\mathrm{pl}} = \frac{\bar{\varepsilon}^{\mathrm{f}+}_{\mathrm{pl}} \cdot \sinh\left(f \cdot (\gamma^{-} - \gamma)\right) + \bar{\varepsilon}^{\mathrm{f}-}_{\mathrm{pl}} \cdot \sinh\left(f \cdot (\gamma - \gamma^{+})\right)}{\sinh\left(f \cdot (\gamma^{-} - \gamma^{+})\right)}, \tag{1}$$

where $\gamma = (1 - k_{\mathrm{sf}} \cdot \eta)/(\tau_{\max}/\bar{\sigma})$ is the shear stress parameter with k_{sf} being the stress triaxiality weight factor, $\tau_{\max}$ being the maximum shear stress and $\bar{\sigma}$ being the von Mises equivalent stress, γ^{-} and γ^{+} are the shear stress parameters at equibiaxial compression and equibiaxial tension, $\bar{\varepsilon}^{\mathrm{f}-}_{\mathrm{pl}}$ and $\bar{\varepsilon}^{\mathrm{f}+}_{\mathrm{pl}}$ are the fracture strains at equibiaxial compresion and equibiaxial tension and f is a model coefficient. The model input parameters are summarized in table 1.

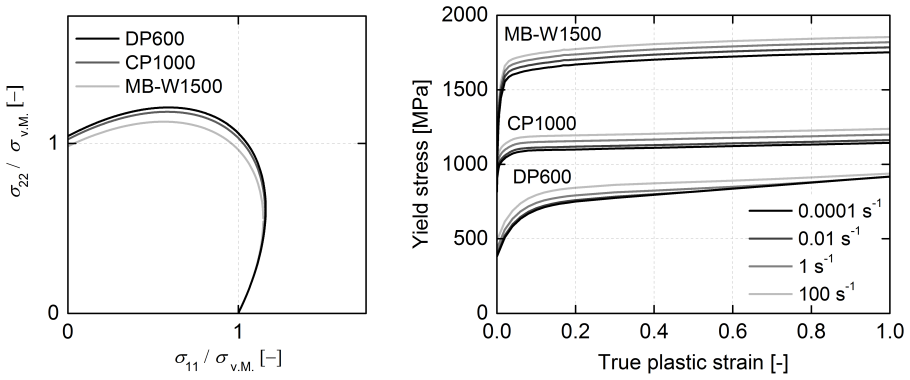


Figure 1. Yield loci (left) and strain-rate-dependent yield curves (right)

Table 1. Coefficients of the CrachFEM ductile shear fracture model [21]

Material	k_{sf}	f	γ^{+}	γ^{-}	$\bar{\varepsilon}_{\mathrm{pl}}^{\mathrm{f}+}$	$\bar{\varepsilon}_{\mathrm{pl}}^{\mathrm{f}-}$
DP600	0.120	2.500	1.840	2.160	0.900	1.900
CP1000	0.202	3.800	1.731	2.269	1.190	7.570
MB-W1500	0.210	0.001	1.720	2.280	0.676	1.543

The ductile normal fracture model was defined as follows:

$$\bar{\varepsilon}_{\mathrm{pl}}^{\mathrm{f}} = d \cdot e^{q\beta}, \tag{2}$$

where $\beta = (1 - k_{\mathrm{nf}} \cdot \eta)/(\sigma_{\mathrm{I}}/\bar{\sigma})$ the normal stress parameter with k_{nf} being the stress triaxiality weight factor and σ_{I} being the first major stress, d is the limit strain magnitude and q is the exponent magnitude. The model input parameters are summarised in table 2.

Table 2. Coefficients of the CrachFEM ductile normal fracture model [21]

Material	k_{nf}	d	q
DP600	0	0.0327	3.430
MB-W1500	0.1515	0.0047	5.517

A comparison of the fracture behaviour descriptions given in figure 2 (plane stress states) and figure 3 (plane strain states) reveals that DP600 and MB-W1500 are characterised by similar fracture strains for low and medium stress triaxialities, whereas MB-W1500 behaves less formable than DP600 at high stress triaxialities. CP1000 possesses a considerably higher level of the fracture strain than the other two materials throughout the whole range of the stress states. It should be noted, however, that the fracture behaviours of the investigated materials were described by different testing laboratories with the help of different testing procedures and evaluation approaches and for this reason should not be compared among one another. From

a comparison of the shear ductile fracture behaviour and normal ductile fracture behaviours for the DP600 and MB-W1500, it can be seen that fracture initiation for these material takes place mainly due to the ductile shear fracture mode at plane stress states. An exception is the equibiaxial stress state ($\eta \approx 0.67$ and $\bar{\theta} \approx -1$) for MB-W1500, at which the ductile fracture mode dominates. At 3D stress states of higher stress triaxialities, the ductile normal fracture mode dominates fracture initiation in DP600 and MB-W1500.

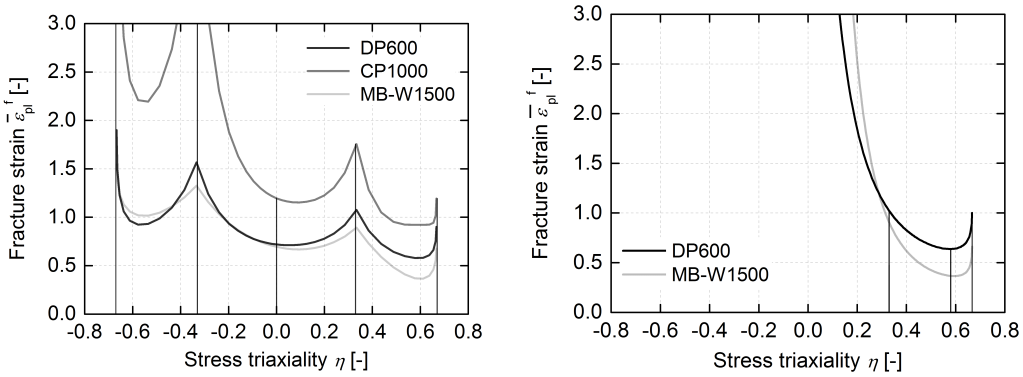


Figure 2. Ductile shear (left) and normal (right) fracture curves for plane stress states

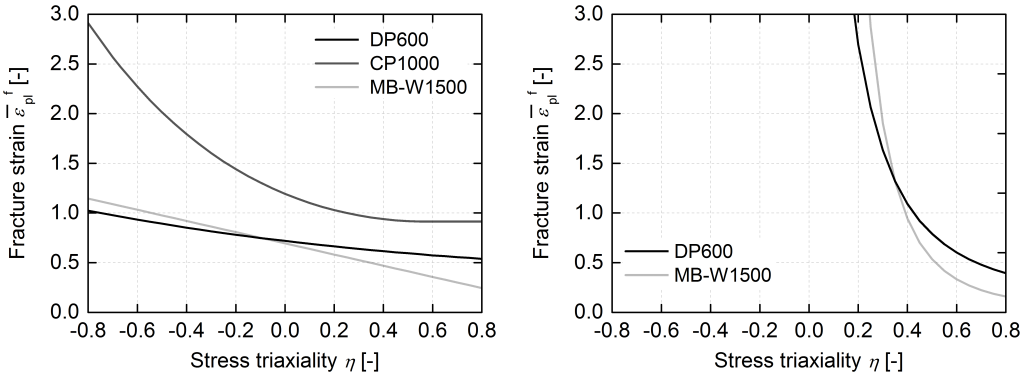


Figure 3. Ductile shear (left) and normal (right) fracture curves for plane strain states

At each increment of the FEA, the incremental equivalent plastic strain $\bar{\varepsilon}_{\mathrm{pl},i}$ in a particular finite element is divided by the fracture strain $\bar{\varepsilon}_{\mathrm{pl}}^{\mathrm{f}}$, which is dependent on the stress state acting in this element during this increment. The division product is accumulated over the increments to obtain the variable D defined by:

$$D = \sum_i \frac{\bar{\varepsilon}_{\mathrm{pl},i}}{\bar{\varepsilon}_{\mathrm{pl}}^{\mathrm{f}}}, \tag{3}$$

which is often referred to as damage variable. At an increment of $D \geq 1$ fracture is assumed. In the present work, the notations D_{s} and D_{n} are used to differentiate between the damage variable according to the shear ductile fracture model and damage variable according to the normal ductile fracture model. From the two, the one is plotted which satisfies $D \geq 1$ first.

3. Finite element modelling

3D volume elements were used to realistically represent the stress state in the material, especially after the onset of plastic strain localisation. In particular, sufficiently fine (approx. 0.1 mm) continuum eight-node linear reduced-integration elements with an hourglass control as provided in the element library of Abaqus/Standard under the notation C3D8R were used for specimen areas of large deformations. To minimise the computation time, the tools which come into contact with the specimen were modelled as rigid bodies.

The in-plane shear tests included shear tests on an ASTM-type specimen, a modified Miyauchi specimen with a one-sidedely reduced thickness [15] and an IFUM butterfly specimen with a one-sidedely reduced thickness (figure 4). The uniaxial tension tests included a bending test on a flanged specimen (figure 5, left) and a tensile test on a holed specimen of 20 mm width and Ø 10 mm hole diameter. The plane strain tension tests included a bending test on a full specimen (figure 5, right) and a tensile specimen of 20 mm width and 5 mm waist radius (the minimum specimen width of 10 mm). Finally, the equibiaxial tension tests encompassed a bulge test with a hemispherical punch of Ø 100 mm and a circular die of Ø 110 mm and R 10 mm and a bulge test with a hemispherical punch of Ø 20 mm and a circular die of Ø 27 mm and R 0.75 mm.

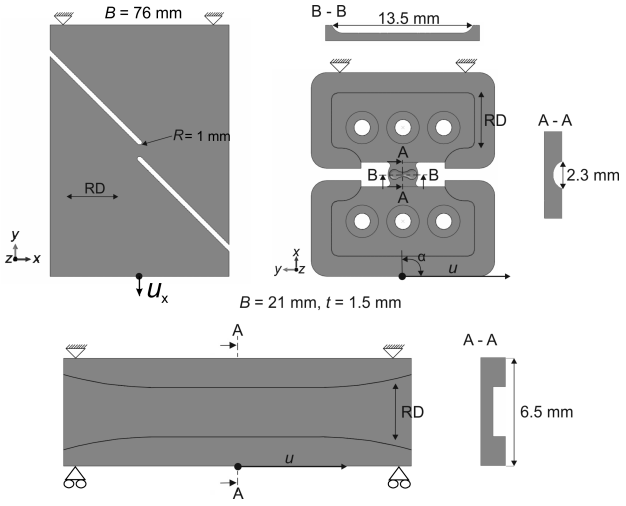


Figure 4. FE models of the in-plane shear tests on the ASTM-type specimen (top left), modified Miyauchi specimen [15] (bottom) and IFUM butterfly specimen with tools (top right)

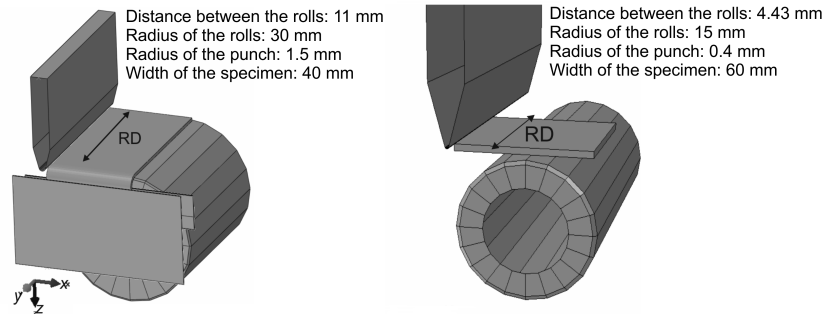


Figure 5. FE models of the bending test on the flanged specimen for uniaxial tension (left) and full specimen for plane strain tension (right)

4. Test evaluation criteria

The tests were evaluated based on ten evaluation criteria. All criteria are related to the distribution of the plastic strain and damage variable as well as the stress state at the location of the crack initiation and are listed below. Next to each criterion a short explanation is given on why this criterion is important and in what case a test is considered to be advantageous according to this criterion.

Defined crack initiation position independent of the material and thickness. The defined crack initiation position independent of the specimen material and thickness reproducibly sucures a desired stress state at the location of the fracture initiation and facilitates development and subsequent application of standard test evaluation procedures, which is considered to be an advantage of a test.

Guarantee of no crack initiation directly at the specimen edge. Especially some of the shear tests are prone to edge cracking, but also other tests like tensile tests on holed and waisted specimen might exhibit edge fracture. The edge fracture can be considered as a premature failure of the specimen. Therefore, it is classified as a disadvantage of a test.

Guarantee of no crack initiation at the machined specimen surface. To avoid edge cracking many researchers suggested new specimen designs with a specimen analysis area of reduced thickness [16], [17], [18]. In most of the cases, the thickness reduction is performed with the help of machining, which might be accompanied by an influence on the material properties [19] and is therefore considered to be a disadvantage of a test.

Variation of the equivalent plastic strain through thickness. A low variation of the equivalent plastic strain through thickness allows a quick and accurate estimation of the fracture strain via a local measurement of the specimen thickness at the point of crack initiation with the help of a sliding calliper or optical microscope and is regarded to be a test advantage.

Variation of the damage variable through thickness. A low variation of the damage variable through thickness allows accounting for the through-thickness scatter of the material formability. As properties variations of sheet metal in its thickness direction are likely due to its manufacturing process, a homogeneous distribution of the damage variable through thickness is advantageous.

Variation of the stress state at the point of crack initiation. A low variation of the stress state at the fracturing material point of the specimen means less uncertainty in the assignment of a characteristic value of the corresponding stress state parameters and is therefore regarded to be an advantage.

Localisation of the plastic strain in the specimen plane. In most of the cases, tests used for characterisation of the sheet metal formability are evaluated with digital image correlation (DIC). A low localisation of the plastic strain in the specimen plane is an important prerequisite for DIC based on the currently available fineness degree of a typical stochastic black-and-white pattern applied to the surface of the specimen, which is seen as an advantage of a test.

Maximum relative difference between the plastic strain at the location of the crack initiation and most deformed point at the surface. A low relative difference between the plastic strain at the location of crack initiation and most deformed material point at the surface, which can be thought of as a measure of the relative error of the fracture strain determination with DIC, is regarded as a test advantage.

Test dependence on the specimen thickness. This collective criterion is related to the dependence of the location of the fracture initiation *and* stress state at the location of fracture initiation on the specimen thickness.

Test dependence on the specimen material. This collective criterion is related to the dependence of the location of the fracture initiation *and* stress state at the location of fracture initiation on the the specimen material.

5. Results and discussion

5.1. In-plane shear tests

The most important advantages of the shear test on an ASTM-type specimen are its non-reduced thickness and low variation of the equivalent plastic strain and damage variable through thickness (figure 6). But these advantages are outweighed by the disadvantages of a possibility of fracture initiation at the specimen edge and a moderate/high variation of the stress state at the point of crack initiation (figure 9, top), which is due to its close proximity to the specimen edge. Furthermore, this test was found to be highly thickness and material dependent (figure 9, top). Even though this test is currently widely used in industry and academia for characterisation of the fracture behaviour of AHSS, it is not universally suitable for this purpose.

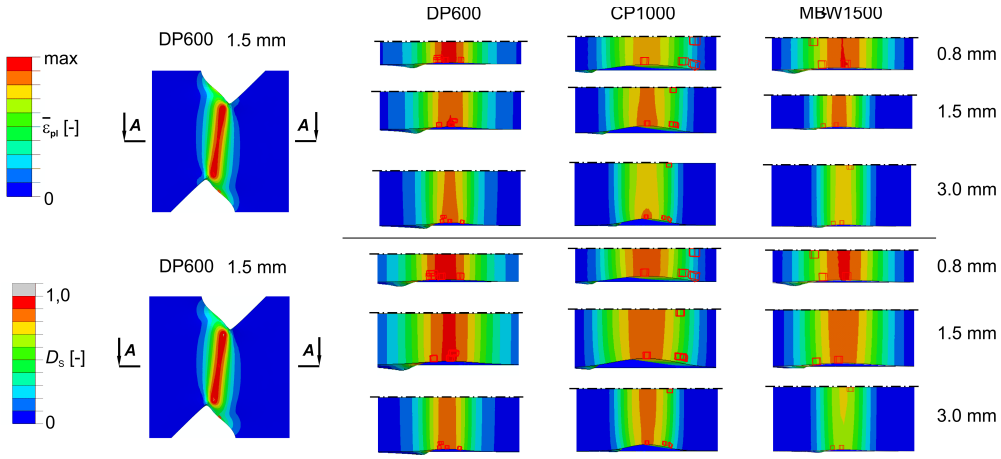


Figure 6. Eq. plastic strain $\bar{\varepsilon}_{\mathrm{pl}}$ (top) and damage variable D_{s} (bottom) in the ASTM-type specimen in the shear test at the moment of crack initiation

In favour of the shear test on the modified Miyauchi specimen [15] speaks the guarantee of no crack initiation at the specimen edge and low maximum relative difference between the plastic strain at the point of crack initiation and most deformed point at the surface (figure 7). The disadvantages include crack initiation at the machined surface and high localisation of the plastic strain in the specimen plane (figure 7). The plastic strain localisation takes place shorty before fracture initiation. Before that, the specimen shows a homogeneous distribution of shear deformation. Therefore, it can be recommended to determine the plastic strain at the onset of this localisation. As the shear test on the ASTM-type specimen, this test was also found to be thickness and material dependent, even though to a substantially lesser degree (figure 9, middle). In summary, this test does not possess the severe disadvantages of the shear test on an ASTM-type specimen and can be recommenden for fracture characterisation of AHSS.

The shear test on an IFUM butterfly specimen with a one-sidedely reduced thickness has an advantage over the other two in-plane shear tests, as its dependency on the specimen thickness and material is negligible (figure 9, bottom). Further advantages include moderate localisation of the plastic strain in the specimen plane and the low maximum relative difference between the plastic strain at the point of crack initiation and most deformed point at the surface (figure 8). The low variation of the stress state at the point of crack initiation and the guarantee of no crack initiation at the specimen edge can be considered as other advantages of this test. To the main disadvantages count the crack initiation at the machined specimen surface and the high variation of the equivalent plastic strain and damage variable through thickness (figure 8). On the whole, this test is not ideal either but it appears to be the best choice among the studied in-plane shear tests.

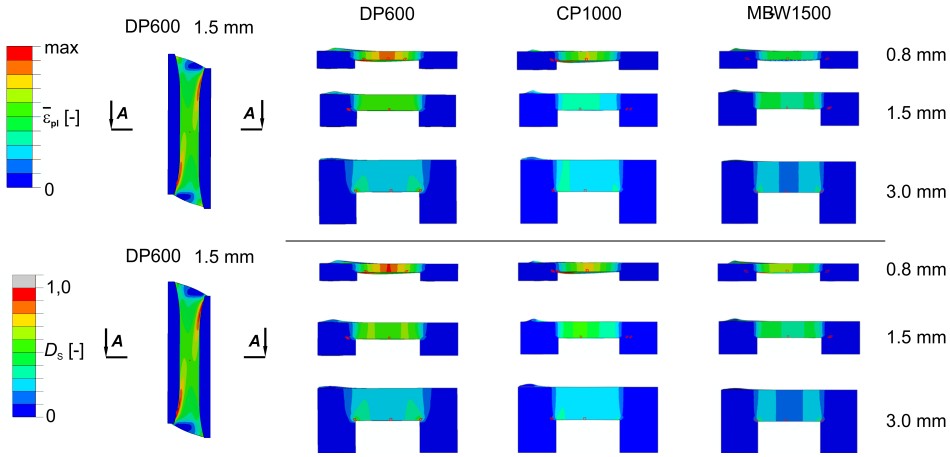


Figure 7. Eq. plastic strain $\bar{\varepsilon}_{\mathrm{pl}}$ (top) and damage variable D_{s} (bottom) in the modified Miyauchi specimen with a one-sidedely reduced thickness [15] in the shear test at the moment of crack initiation

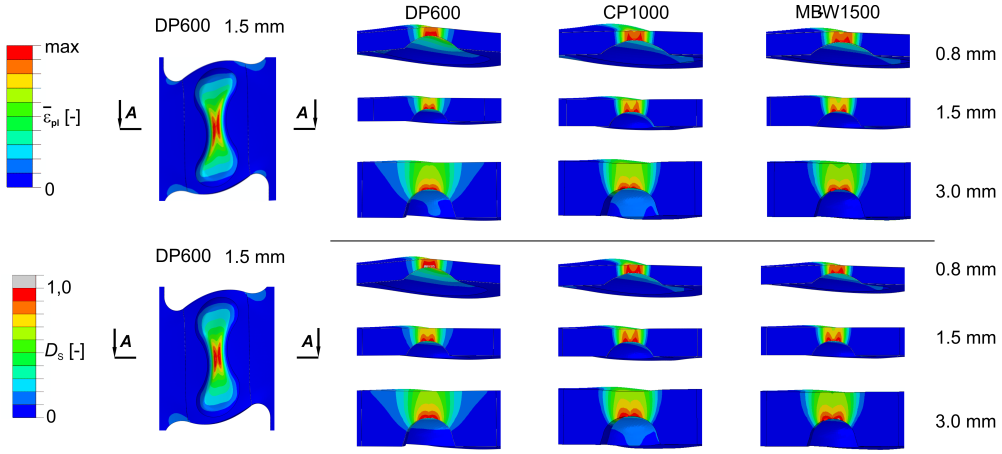


Figure 8. Eq. plastic strain $\bar{\varepsilon}_{\mathrm{pl}}$ (top) and damage variable D_{s} (bottom) in the IFUM butterfly specimen with a one-sidedely reduced thickness in the shear test at the moment of crack initiation

5.2. Uniaxial tension tests

From the two studied tests, the tensile test on a holed specimen has an advantage over the three-point bending test on a flanged specimen, as it guarantees no crack initiation directly at the edge (figure 10 and figure 11). On the contrary, the three-point bending test on a flanged specimen has an advantage over the tensile test on a holed specimen, as it possesses a lower variation of the damage variable through thickness and can therefore better account for possible scatter of the material formability in the thickness direction (figure 10). Furthermore, the three-point bending test on a flanged specimen excels the tensile test on a holed specimen with its slightly lower variation of the stress state at the material point of crack initiation for a given material (figure 12) and a slightly lower localisation of the plastic strain in the specimen plane (figure 10 versus figure 11). Also, the maximum relative difference between the plastic strain at the point of crack initiation and most deformed point at the surface for all materials and thicknesses was found smaller for the three-point bending test on a flanged specimen. The thickness dependency

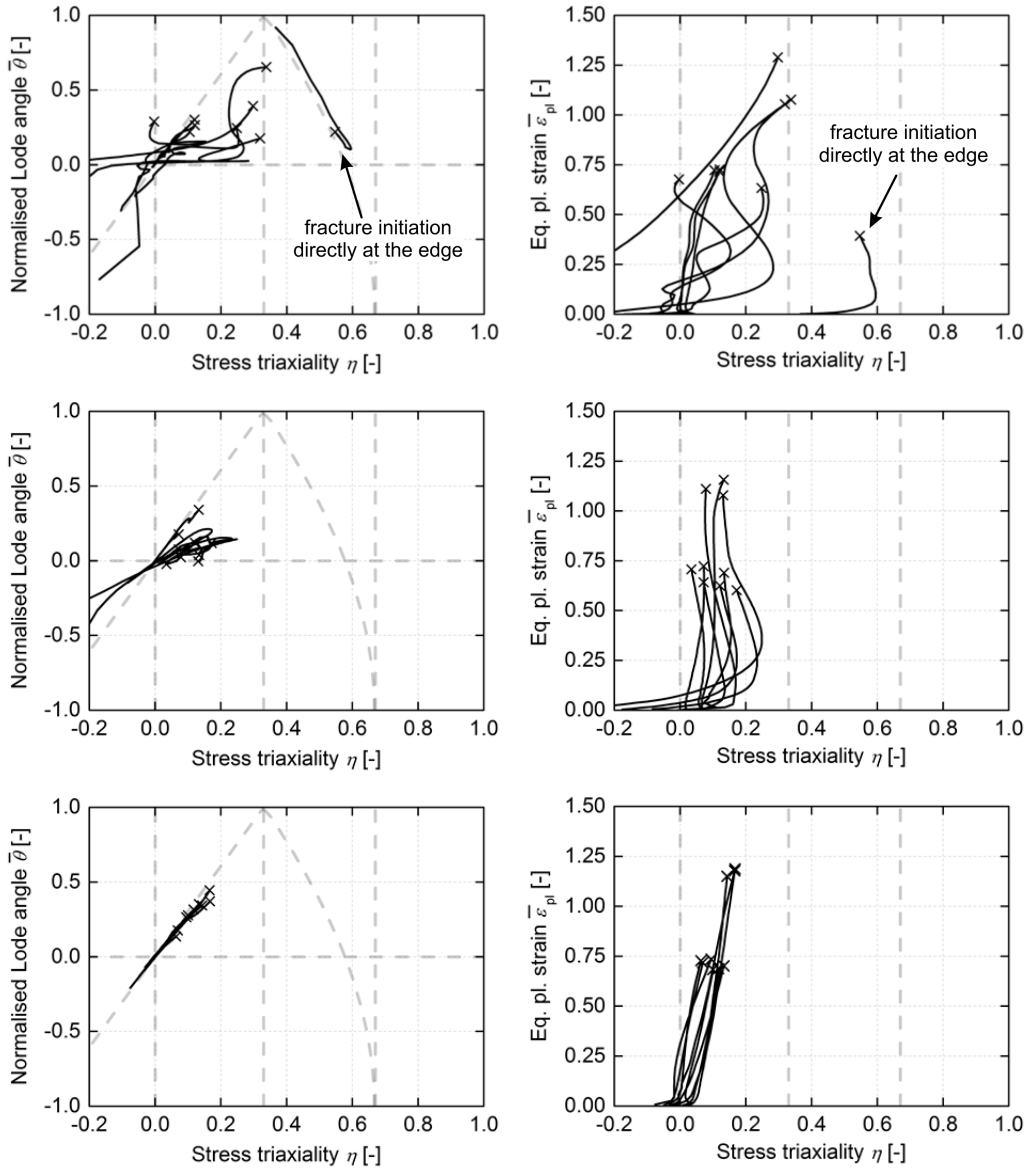


Figure 9. Stress state at the location of fracture initiation in the ASTM-like specimen (top), modified Miyauchi specimen (middle) and IFUM butterfly specimen (bottom) in the shear test for all combinations of the materials and thicknesses each

of the three-point bending test on a flanged specimen was found to be on average lower than for the tensile test on a holed specimen. On the contrary, the latter test performs better what material dependency concerns. To sum up, the tensile test on a holed specimen performs more reproducibly for various materials and thicknesses providing a good safety against edge cracking and a tolerable difference between the equivalent plastic strain at the material point of fracture initiation and most deformed material point at the surface and is considered to be the better choice in the present study even though it does not accurately enough model the stress state of uniaxial tension.

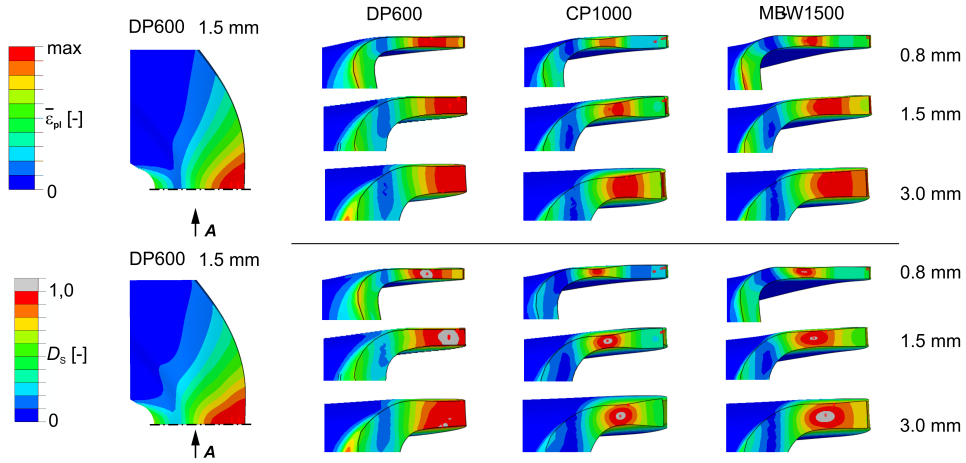


Figure 10. Eq. plastic strain $\bar{\varepsilon}_{\mathrm{pl}}$ (top) and damage variable D_{s} (bottom) in the flanged specimen in the three-point bending test at the moment of crack initiation

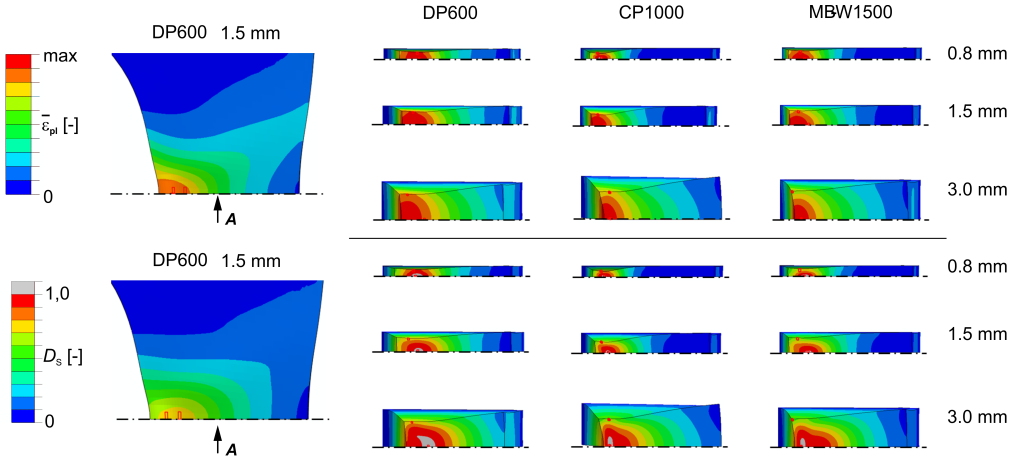


Figure 11. Eq. plastic strain $\bar{\varepsilon}_{\mathrm{pl}}$ (top) and damage variable D_{s} (bottom) in the holed specimen in the tensile test at the moment of crack initiation

5.3. Plane strain tension tests

For thicker materials, the advantages of the three-point bending test on the full specimen outweigh the advantages of the tensile test on the waisted specimen, especially what the stress state concerns (figure 15). However, for ductile materials and low thicknesses, no fracture is achieved at the bending radius, which compromises the test universality. Disregarding the specimen thickness, the three-point bending test on the full specimen possesses a high variation of the damage variable through thickness. In this respect, the tensile test on a waisted specimen delivers better results. But it reveals a high variation of the stress state at fracturing material point. For some materials, like DP600 and MB-W1500 of this study, this may lead to fracture initiation in the ductile normal fracture mode, which is a disadvantage if the test is to be used to characterise ductile shear fracture. On the whole, however, the tensile test on the waisted specimen is found more suitable and more universal for fracture characterisation of AHSS. But for characterisation of shear fracture, its optimisation or an alternative test is required.

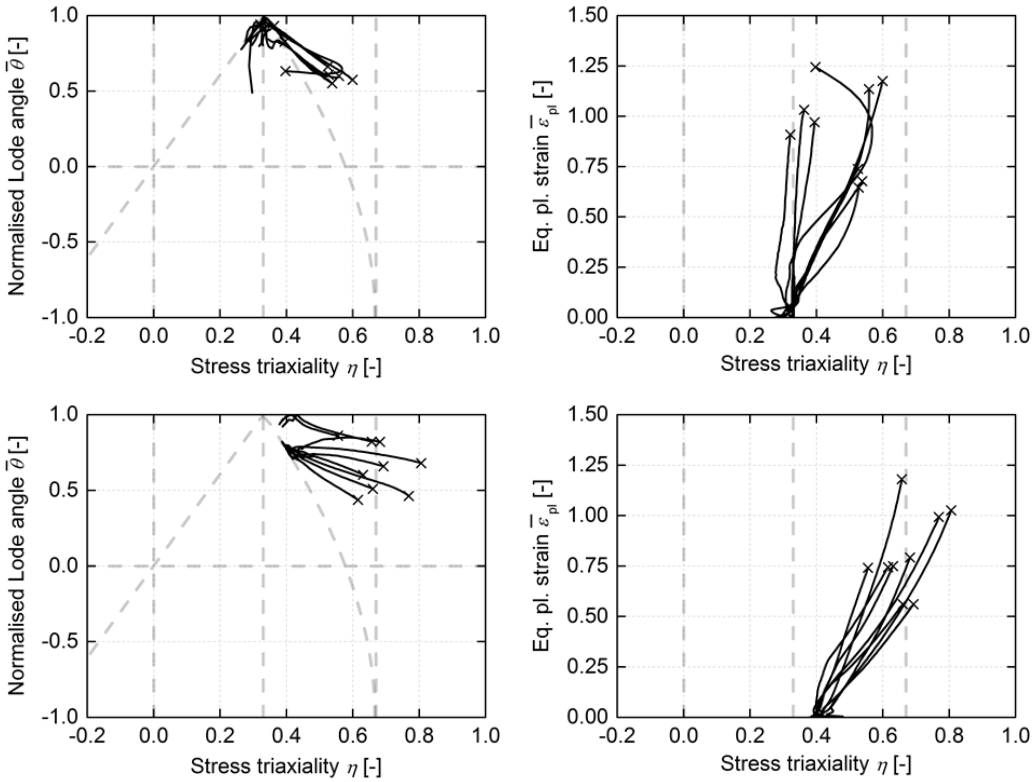


Figure 12. Stress state at the location of fracture initiation in the flanged specimen in the three-point bending test (top) and holed specimen in the tensile test (bottom) for all combinations of the materials and thicknesses each

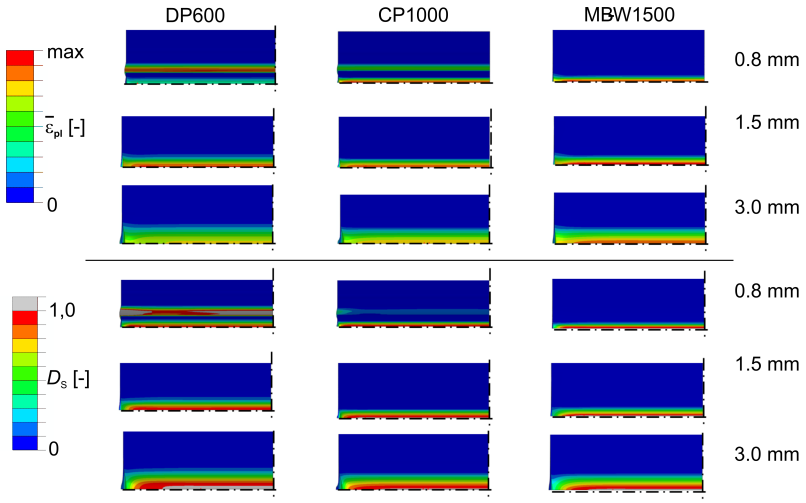


Figure 13. Eq. plastic strain $\bar{\varepsilon}_{\mathrm{pl}}$ (top) and damage variable D_{s} (bottom) in the full specimen in the three-point bending test at the moment of crack initiation

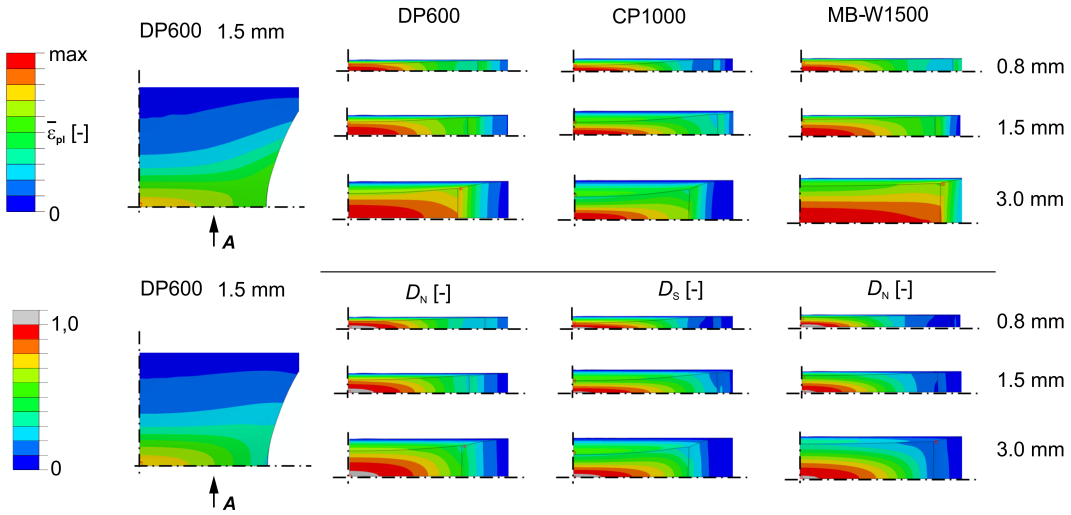


Figure 14. Eq. plastic strain $\bar{\varepsilon}_{\mathrm{pl}}$ (top) and damage variable D_{s} or D_{n} (bottom) in the waisted specimen in the tensile test at the moment of crack initiation

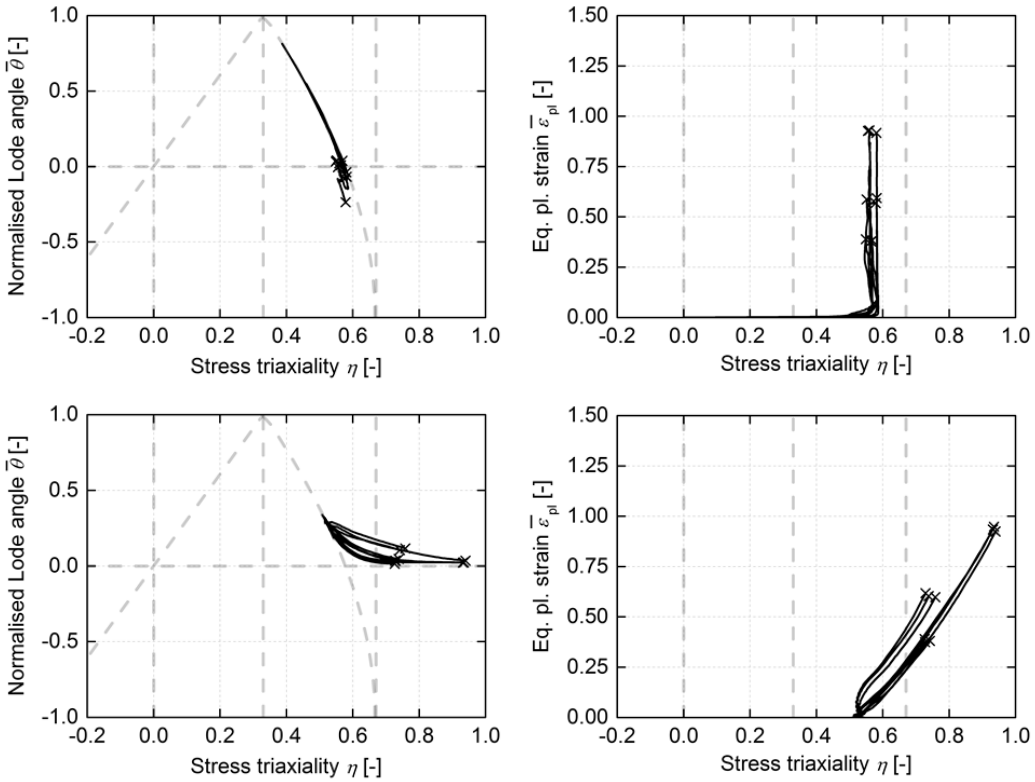


Figure 15. Stress state at the location fracture initiation in the full specimen in the three-point bending test (top) and waisted specimen in the tensile test (bottom) for all combinations of the materials and thicknesses

5.4. Equibiaxial tension tests

Contrary to the previously described test groups, the more favourable test exists in this group, with its advantages overweighing the advantages of its group counterpart: the bulge test with a punch of Ø 100 mm. It is well suitable for the fracture strain determination both with the help of thickness measurement and DIC. Furthermore, the test assures crack initiation at a defined position at the pole of the bulge or in its immediate proximity (figure 16) and delivers a constant stress state independent of the specimen thickness and material (figure 18, top). For DP600 and CP1000 ductile shear fracture occurs. For MB-W1500, ductile normal fracture leads to the specimen failure, though $D_\mathrm{n} \approx D_\mathrm{s}$. Contrary to that, the bulge test with a punch of Ø 20 mm was found to have a moderate dependency on the specimen thickness, which leads to a disadvantageous variation of the crack initiation position (figure 17) and stress state (figure 18, bottom). Moreover, notable gradients of the equivalent plastic strain and damage variable through thickness for thicker specimens in this test take place (figure 17), which reduce the accuracy of the fracture strain determination via the thickness measurement and hinder accounting for possible scatter of the material formability in the thickness direction.

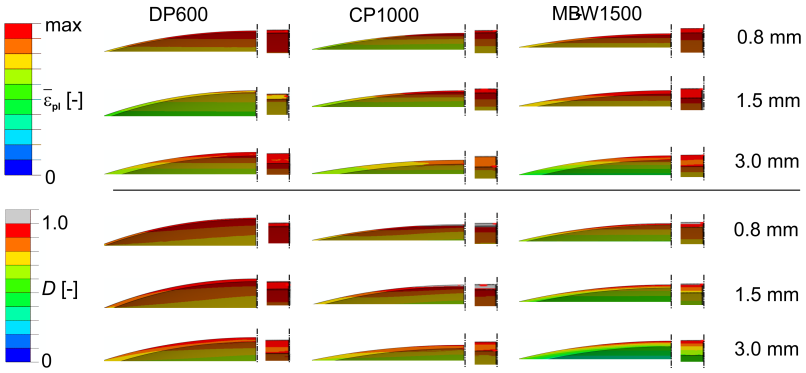


Figure 16. Eq. plastic strain $\bar{\varepsilon}_\mathrm{pl}$ (top) and damage variable D_s or D_n (bottom) in the circular specimen in the bulge test with a punch of Ø 100 mm at the moment of crack initiation

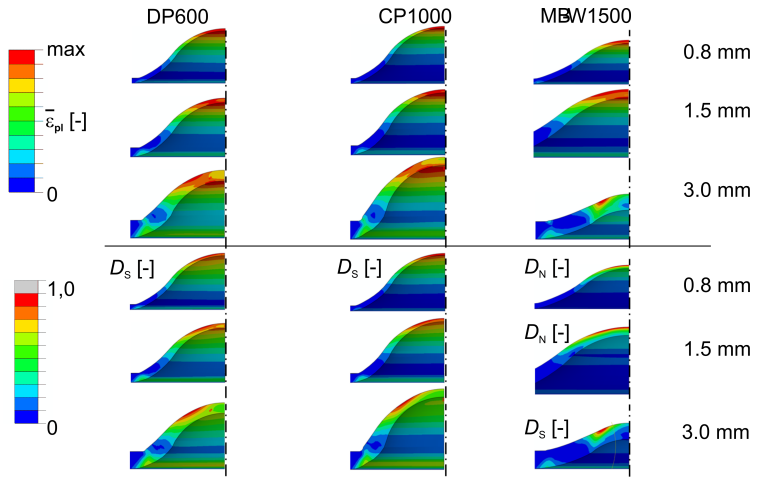


Figure 17. Eq. plastic strain $\bar{\varepsilon}_\mathrm{pl}$ (top) and damage variable D_s or D_n (bottom) in the circular specimen in the bulge test with a punch of Ø 20 mm at the moment of crack initiation

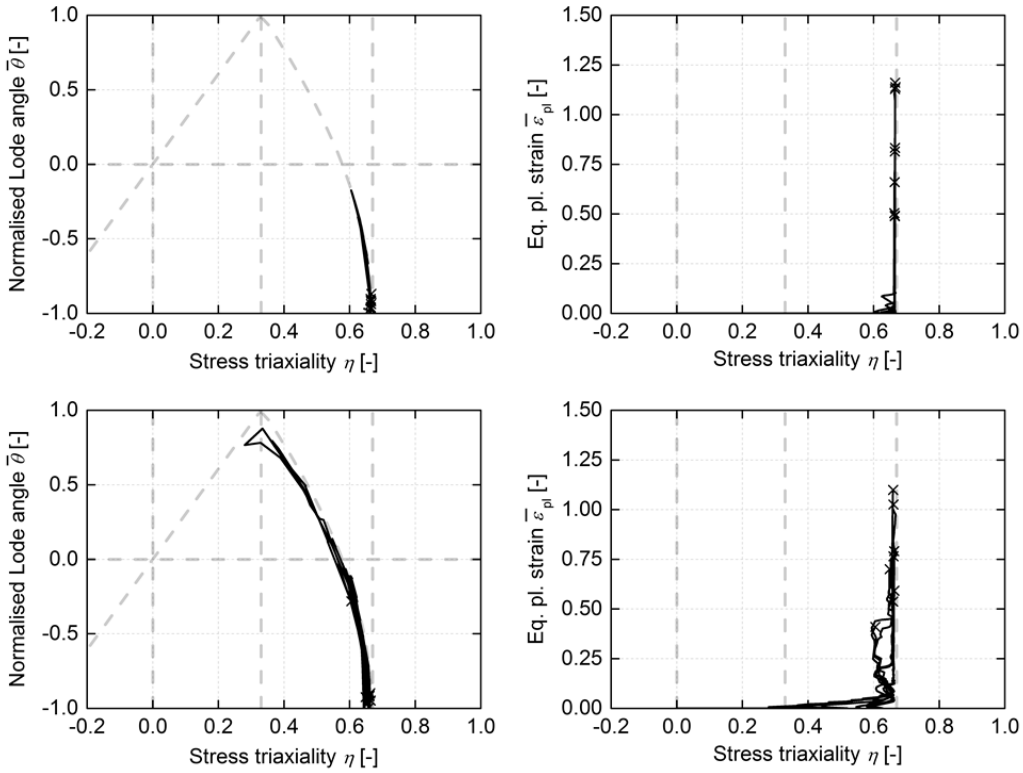


Figure 18. Stress state at the location of fracture initiation in the circular specimen in the bulge test with a punch of Ø 100 mm (top) and circular specimen in the bulge test with a punch of Ø 20 mm (bottom) for all combinations of the materials and thicknesses

5.5. Summary

The test analysis reveals that all the investigated tests have their advantages and disadvantages (table 3). For in-plane shear, uniaxial tension and plane strain tension, no test can be unconditionally recommended as its disadvantages cannot be neglected. However, in each of these groups, a test can be chosen, which represents an acceptable compromise between its advantages and disadvantages: the shear test on an IFUM butterfly specimen for in-plane shear, the tensile test on a holed specimen for uniaxial tension, the tensile test on a waisted specimen for plane strain tension. For equibiaxial tension, the bulge test on a circular specimen with a punch of Ø 100 mm (alternatively, a hydraulic bulge test [20]) can be unconditionally recommended. The results of the shear test on an IFUM butterfly specimen, tensile test on a holed specimen, tensile test on a waisted specimen and bulge test on a circular blank with a punch of Ø 100 mm are summarised in figure 19. It can be seen that these tests provide a basis for characterisation of the fracture behaviour of AHSS in a range of practice-relevant stress states.

6. Conclusion and outlook

The paper presents results of evaluation of different commonly available tests for fracture characterisation of AHSS with the help of the FEA. For in-plane shear, uniaxial tension and plane strain tension, no test can be unconditionally recommended as disadvantages of all studied tests in these groups cannot be neglected. However, in each of these groups, a test can be chosen, which represents an acceptable compromise between its advantages and disadvantages: the shear test on an IFUM butterfly specimen for in-plane shear, the tensile test on a holed

Table 3. Summary of the test results according to the test evaluation criteria

		Defined crack initiation position independent of the material and thickness	Guarantee of no crack initiation directly at the specimen edge	Guarantee of no crack initiation at the machined specimen surface	Variation of the equivalent plastic strain through thickness	Variation of the damage variable through thickness	Variation of the stress state at the point of crack initiation	Localisation of the plastic strain in the specimen plane	Max. relative difference between the plastic strain at the point of crack initiation and most deformed point at the surface	Test dependence on the specimen thickness	Test dependence on the specimen material
in-plane shear	Shear test on the ASTM-type spec.	no	no	yes	low	low	moderate/ high	low/ moderate	high	high	high
	Shear test on the mod. Miyauchi-type spec.	no	yes	no	moderate	moderate	moderate	high	low	moderate	moderate
	Shear test on an IFUM butterfly-type spec.	yes	yes	no	high	high	low	moderate	low	low	low
unia. tension	Three-point bending test on a flanged spec.	no	no	yes	low/ moderate	low/ moderate	low/ moderate	low/ moderate	moderate	low/ moderate	high
	Tensile test on a holed spec.	no	yes	yes	moderate/ high	moderate	moderate	moderate	moderate/ high	high	moderate
plane strain	Three-point bending test on a full spec.	yes	yes	yes	high	high	low	moderate/ high	low	low	low
	Tensile test on a waisted spec.	yes	yes	yes	moderate/ high	moderate/ high	moderate/ high	low/ moderate	high	low/ moderate	low/ moderate
bia. tension	Bulge test with a punch ∅ 100	yes	yes	yes	low/ moderate	low/ moderate	low	low	low	low	low
	Bulge test with a punch ∅ 20	no	yes	yes	moderate/ high	moderate/ high	moderate	low	low	moderate	low

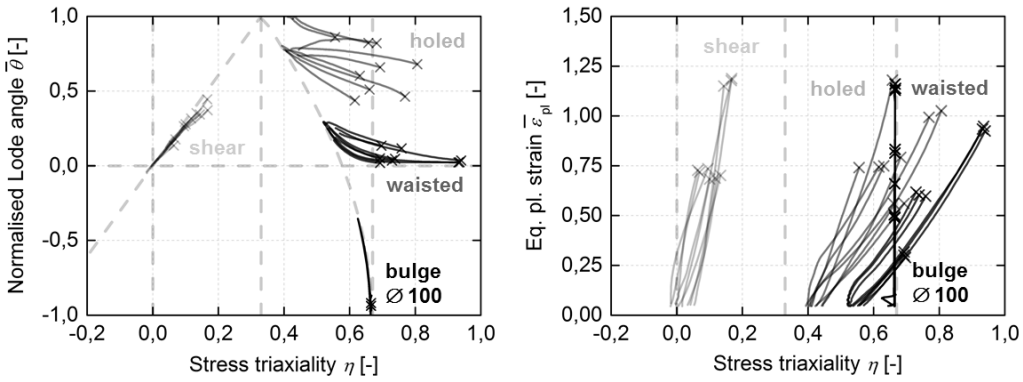


Figure 19. Stress state at the fracture initiation location the preferred specimens

specimen for uniaxial tension, the tensile test on a waisted specimen for plane strain tension. On the contrary, the bulge test on a circular specimen with a punch of Ø 100 mm can be unconditionally recommended for equibiaxial tension. Together, these four tests provide a basis for fracture characterisation of AHSS. In the future, optimisation of the studied tests for in-plane shear, uniaxial tension and plane strain tension appears to be necessary. In particular, the IFUM butterfly specimen could be optimised for a more homogeneous distribution of plastic deformation through thickness, the holed specimen could be optimised to better model uniaxial tension and the waisted specimen could be optimised to induce shear instead of normal fracture.

Acknowledgments
The project P 1145 "Test evaluation" [21] of the Research Association for Steel Application (FOSTA), Germany, was initiated by the Working group "Characterisation of damage models" of the Materials committee of the Steel Institute VDEh, Germany. The financial support by the FOSTA is gratefully acknowledged. The authors also thank the members of the project committee Dr. P. Dietsch (ArcelorMittal S. A.), Dr. H. Friebe (Gesellschaft für optische Messtechnik mbH), Dr. H. Gese (MATFEM Partnerschaft Dr. Gese & Oberhofer), Dr. B. Hackl (voestalpine Stahl GmbH), Dr. H. Richter and H. Rösen (ThyssenKrupp Steel Europe AG), M. Schneider (Salzgitter Mannesmann Forschung GmbH) and Dr. C. ten Horn (Tata Steel Europe Ltd.) for the provided material models, test details and valuable comments.

References

[1] Heuss R, Müller N, van Sintern W and Starke A 2012 *Lightweight, heavy impact* (McKinsey & Company)
[2] Banabic D 2010 *Sheet Metal Forming Processes. Const. Modelling and Num. Simulation* (Berlin: Springer)
[3] Roll K 2008 Simulation of sheet metal forming – necessary developments in the future *Proc. Int. Conf. and Workshop on Num. Sim. of 3D Sheet Metal Forming Processes (Interlaken)* (Zurich: IVP, ETH) pp 3-11
[4] Keßler L and Gerlach J 2008 Industrial aspects of material modelling for steel grades in the past, present and future *Proc. Int. Conf. and Workshop on Num. Sim. of 3D Sheet Metal Forming Processes (Interlaken)* (Zurich: IVP, ETH) pp 13-17
[5] Bao Y and Wierzbicki T 2004 A comparative study on various ductile crack formation criteria *J. Eng. Mater. Technol.* **126** pp 314-24
[6] Hooputra H, Gese H, Dell H and Werner H 2004 A comprehensive failure model for crashworthiness simulation of aluminium extrusions *Int. J. Crash.* **9** pp 449-63
[7] Wierzbicki T, Bao Y, Lee Y-W and Bai Y 2005 Calibraton and evaluation of seven fracture models *Int. J. Mech. Sci.* **47** pp 719-43
[8] Till E and Hackl B 2013 Calibration of plasticity and failure models for AHSS sheets *Proc. IDDRG Conf. (Zurich)* (Zurich: Institute of Virtual Manufacturing, ETH) pp 119-24
[9] Bai Y and Wierzbicki T 2013 The concept of damage accumulation for prediction necking and fracture of sheets *Proc. IDDRG Conf. (Zurich)* (Zurich: Institute of Virtual Manufacturing, ETH) pp 9-13
[10] Walters CL 2009 Development of a punching technique for ductile fracture testing over a wide range of stress states and strain rates *PhD Thesis* (Cambridge: MIT)
[11] Chottin J, Hug E and Rachnik M 2011 Damage accumulation in DP1000 sheets submitted to various stress states *Steel Res. Int.* **Spec. Ed. ICTP Conf.** pp 895-900
[12] Behrens B-A, Bouguecha A, Vucetic M and Peshekhodov I 2012 Characterisation of the quasi-static flow and fracture behaviour of DP steel sheets in a wide range of stress states *Arch Civ Mech Eng* **12** pp 397-406
[13] Behrens B-A, Vucetic M and Peshekhodov I 2014 Effiziente Charakterisierung und Modellierung des Fließ- und Versagensverhaltens von Dualphasenstählen *Tagungsband des Umformtechnischen Kolloquiums Hannover* (Hanover: IFUM, Leibniz Universität Hannover) pp 77-97
[14] Keßler L, Richter H and Rösen H 2014 Die Anwendung von erweiterten Bewertungskriterien für die Simulation von Stahlwerkstoffen *Tagungsband des Umformtechnischen Kolloquiums Hannover* (Hanover: IFUM, Leibniz Universität Hannover) pp 99 -109
[15] Partnerschaft Dr. Gese & Oberhofer 2016 *www.matfem.de*
[16] Mohr D and Henn S 2007 Calibration of stress-triaxiality dependent crack formation criteria: a new hybrid experimental-numerical method *Exp. Mech.* **47** pp 805-20
[17] Bai Y 2008 Effect of loading history on necking and fracture *PhD thesis* (Cambridge: MIT)
[18] Behrens B-A, Vucetic M and Peshekhodov I 2014 Calibration of fracture initiation models for advanced high-strength sheet steels in a wide range of stress states using a uniaxial tensile testing machine *Proc. IDDRG Conf. (Paris)* (Senlis Cedex: CETIM) pp 252-57
[19] Behrens B-A, Vucetic M and Peshekhodov I 2015 *Methode zur Charakterisierung des Versagensverhaltens hochfester Stahlblechwerkstoffe in einem breiten Spektrum von Spannungszuständen mithilfe einachsig arbeitender Zugprüfmaschinen* (Dusseldorf: Verlag und Vertriebsgesellschaft mbH)
[20] Vucetic M, Bouguecha A, Peshekhodov I, Götze T, Huinink T, Friebe H, Möller T and Behrens B-A 2011 Num. validation of analytical biaxial true stress - true strain curves from the bulge test *Proc. Int. Conf. and Workshop on Num. Sim. of 3D Sheet Metal Forming Processes (Seoul)* (Melville: AIP) pp 107-14
[21] Behrens B-A and Peshekhodov I 2016 *Evaluation of common tests for fracture characterisation of advanced high-strength sheet steels with the help of the finite element analysis* (Dusseldorf: Verlag und Vertriebsgesellschaft mbH)